JSEE Vol. 22, No. 3, 2020 DOI:10.48303/jsee.2020.251304

Research Paper

Retrospective Estimation of the Hypocentre and Possible Early Warning for the November 12, 2017 Mw 7.3 Sarpol-e Zahab Earthquake in Western Iran

Kianoush Rostami[1], Sajad Mirzaei[1], John Douglas[2], and Alireza Azarbakht[3,4,5]*

1. M.Sc. Graduate, Department of Civil Engineering, Faculty of Engineering, Arak University, Arak, Iran
2. Senior Lecturer, Department of Civil and Environmental Engineering, University of Strathclyde, Glasgow, UK
3. Associate Professor, Department of Civil Engineering, Faculty of Engineering, Arak University, Arak, Iran
4. Research Fellow, Department of Civil and Environmental Engineering, University of Strathclyde, Glasgow, UK
5. Lecturer, University of Greenwich, School of Engineering, Kent, UK,
*Corresponding Author; email: a.azarbakht@greenwich.ac.uk

Received: 14/12/2021
Revised: 01/03/2022
Accepted: 04/04/2022

ABSTRACT

An effective Earthquake Early Warning System (EEWS) has to provide accurate estimates of the location and magnitude of an earthquake that has the potential to cause destructive ground motions. All this must happen within a few seconds after the first P-wave is detected by recording stations and before the arrival of strong S and surface waves. The largest earthquake (Mw 7.3) of the past century in the Zagros region (Iran) occurred on November 12, 2017 and was felt in several neighbouring countries; nevertheless, no EEWS was operating in the region. In this short article, an evolutionary real-time location estimation method (but retrospectively examined in the current study) based on the combination of the Voronoi diagram and Kalkan [1-3] algorithms has been used to simulate the potential of an EEWS to estimate the Sarpol-e Zahab earthquake's hypocentre. The employed algorithms use information on the successive triggering of stations by the P wave, from the first station (for which the estimate has low accuracy) up to a maximum of three stations (for which the estimate has acceptable accuracy). The depth of the earthquake is then determined using the arrival time of the S wave. The estimated hypocentre is in good agreement with offline reports by BHRC [4]. Moreover, an EEWS would ensure a meaningful warning time. As the main finding of the present study, for many locations and major cities, a time alert of more than 20 s for strong shaking (macroseismic intensity VI or above) locations and many tens of seconds for weaker shaking are estimated. Therefore, the establishment of an EEWS should be encouraged to improve the resilience of this region of high seismic hazard.

Keywords:
Earthquake early warning system; Voronoi diagram; BHRC; P-wave

1. Introduction

The establishment of an EEWS is a relatively new concept for reducing earthquake risk and increasing resilience to seismic hazards, particularly in urban regions [5]. An EEWS provides real-time information about earthquakes, enabling individuals, communities, governments, businesses, and others located at an appropriate distance to take timely action to reduce the probability of harm. An EEWS could help to reduce financial losses and mitigate injuries or death. These systems are currently

operating in nine countries (USA, Japan, Mexico, Romania, Turkey, Taiwan, South Korea, China and India), and also are being tested for implementation in many others [5]. No operational EEWS has yet been implemented in Iran or neighbouring countries; although, the concept of EEWS had been published by a telegraph operator in a Persian newspaper in 1909 [6] and some past studies have demonstrated the feasibility of EEWS in Iran [7-9].

EEWSs use the advantage of the much faster propagation of electromagnetic waves as compared to seismic waves to provide a short, but potentially useful, warning time beyond the blind zone. In an EEWS, seismic stations need to be located with appropriate density in the area where destructive earthquakes are likely to happen. Then shortly after the devastating earthquake, estimates of the earthquake's magnitude and location can be sent to the sites likely to be affected by the earthquake before the destructive seismic waves arrive. A successful example is Japan's high-speed train EEWS [10], which triggered, for example, in October 2004 after detecting a magnitude 6.6 earthquake. The automatic brakes activated after a short time and stopped a high-speed train, travelling at around 200 km/h, before the strong shaking arrived [11].

On November 12, 2017, an Mw 7.3 earthquake occurred at 18:18:16 UTC (21:48:16 local time) in Kermanshah county in Iran [12-13]. The earthquake has been the largest event in the Zagros region since the M 7.4 1909 Silakhor earthquake [13]. 109 stations (with SSA-2 and CMG5TD instruments) of the Iran Strong-Motion Network operated by BHRC (Figure 1) recorded strong ground motions from this earthquake in Iran's western and central provinces [4]. A maximum peak ground acceleration (based on unprocessed data) of 0.7 g was recorded at the Sarpol station [13]. The earthquake shaking was felt in many different countries, including Iran, Iraq, Syria, Saudi Arabia, Armenia, Jordan, Egypt, Qatar, Bahrain, the United Arab Emirates and Turkey (see Figure 2). The distribution of the Modified Mercalli Intensity (MMI), reported by the USGS [14], is shown in Figure (2). MMI equal to or greater than V (moderate shaking) was observed as far as 100 km from the earthquake's epicentre. The widespread occurrence of high MMI intensities

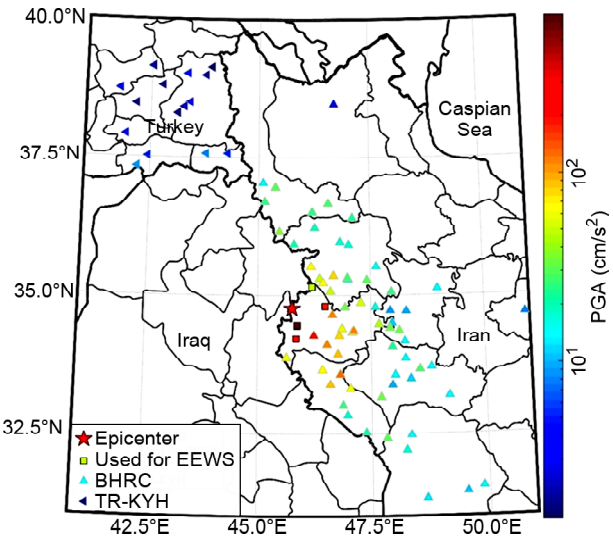

Figure 1. Stations that recorded ground accelerations of the Mw 7.3 Sarpol-e Zahab, Iran-Iraq Earthquake. The right colour bar indicates the level of recorded PGA in each station.

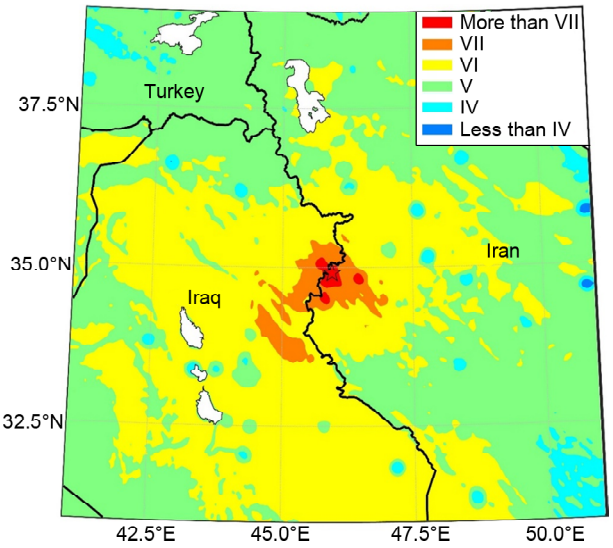

Figure 2. MMI isoseismal map based on USGS data for the Mw 7.3 Sarpol-e Zahab, Iran-Iraq Border Earthquake [14].

in several neighbouring countries suggests that establishing an EEWS in the region would be beneficial.

As real-time estimation of an earthquake's epicentre and depth play a crucial role in a well-designed EEWS, in this short article, we investigate whether the current seismic network could provide sufficient warning times for the region. We believe that this is the first time that such a study has been made for the considered region. In the next section, a real-time framework (but retrospectively demonstrated in this study) for the estimation of the epicentre and depth is introduced by using waveforms from the first stations that recorded the

earthquake. Subsequently, a hypothetical EEWS in the region is proposed, and warning times are estimated. Finally, some practical conclusions are drawn.

2. Earthquake Location Estimation

Many researchers have proposed real-time techniques to estimate earthquake locations. For example, Anderson [15] proposed an algorithm for the real-time location of earthquakes based on the sequence of station arrival times. Kanamori [16] proposed a real-time location algorithm using the attenuation of seismic amplitudes; however, this algorithm has not been used for a real-time EEWS. The "Master Station" theory was proposed by Zhou [17], which was a major advance, and this method has been used in many subsequent studies. Other methods include the "B-Δ" model proposed by Odaka et al. [18], which is applied in the EEWS of Japan and has been studied for an EEWS in Iran [8]. The concept of "Two-Station Subarray" proposed by Rydelek and Pijol [19] is also considered for EEW. They believe that a highly accurate result is not as important as the speed of processing. The "not-yet arrival" method proposed by Horiuchi et al. [20] is unique since this method makes full use of the information received by the stations and uses those stations that have not yet been triggered to determine the location of the earthquake. Satriano et al. [21] used Horiuchi's method and combined it with a probability density function to indicate the spot of maximum probability as the epicentre. Ma [22] conducted studies on EEWS location methods, including the Voronoi diagram, Delaunay triangulation, station azimuth, and two-station hyperbolic method.

The speed and accuracy of the earthquake location method directly impact the success of any employed EEWS. In Japan, for example, several seismic and geodetic sensors were installed in the Pacific Ocean to allow an earlier and more accurate detection of strong offshore events [23]. There will always be a compromise between the number of stations considered, the chance of a false alarm and the length of the warning time. For example, Grasso et al. [24] showed that the error in magnitude estimation is 0.7 units when only one station is used. This error can be decreased to 0.6, 0.45 or 0.35 units when three, five or ten stations are considered [25]. The more recording stations are used for an EEWS, the shorter the warning time and the wider the blind zone of the EEWS will be. Hence, the use of a precise, fast, fixed, and reliable (real-time) location method is required for this purpose. In the current study, a method based on the Voronoi diagram [26] is employed. The continuous evolution of the earth-quake location estimate is determined by gradually reducing the area using information on which stations have observed a *P* wave. First, we divide the area of the seismic network into subdivisions using the Voronoi diagram method (see Figure 3a), and then we go through the steps described in the following section. It should be noted that, in the present study, the S-wave velocity and the average Vp/Vs ratio for the study region are, respectively, assumed to be 3.6 km/s and 1.8 [27-28]. Therefore, the P-wave velocity is considered equal to 6.3 km/s.

2.1. Locating the Epicentre Considering the First Station to Receive the P Wave

To meet the requirements of an EEWS, accurate information on the operational status of the stations is required. In such a way, the abnormal/non-operational stations are identified and eliminated in advance. Then according to the available operational stations, we draw the Voronoi diagram (Figure 3b). However, feeding real-time data into an operational EEWS platform is always a challenging task. In this case, each station has its subdivision. Figure (3b) shows the seismic network in the region of the Sarpol-e Zahab earthquake. If each station is operational (no station is offline nor broken), then the control area of each station in this network is divided into smaller areas using the Voronoi subdivision. The boundaries are vertical perpendicular lines between the two adjacent stations, as marked in Figure (3b). When the first station within this network observes the *P* wave (t_{P1}) (the black triangle in Figure 3b), the epicentre can only be located inside that station's subdivision.

In Figure (3b), (x, y), (x_{S1}, y_{S1}), and (x_{S2}, y_{S2}) are the actual epicentre (unknown), the coordinates of the first triggered station (known), and the coordinates of the second triggered station (known), respectively. The earthquake depth, *h*, is estimated as the average depth of earthquakes with a magnitude greater than 3 in the study region in the

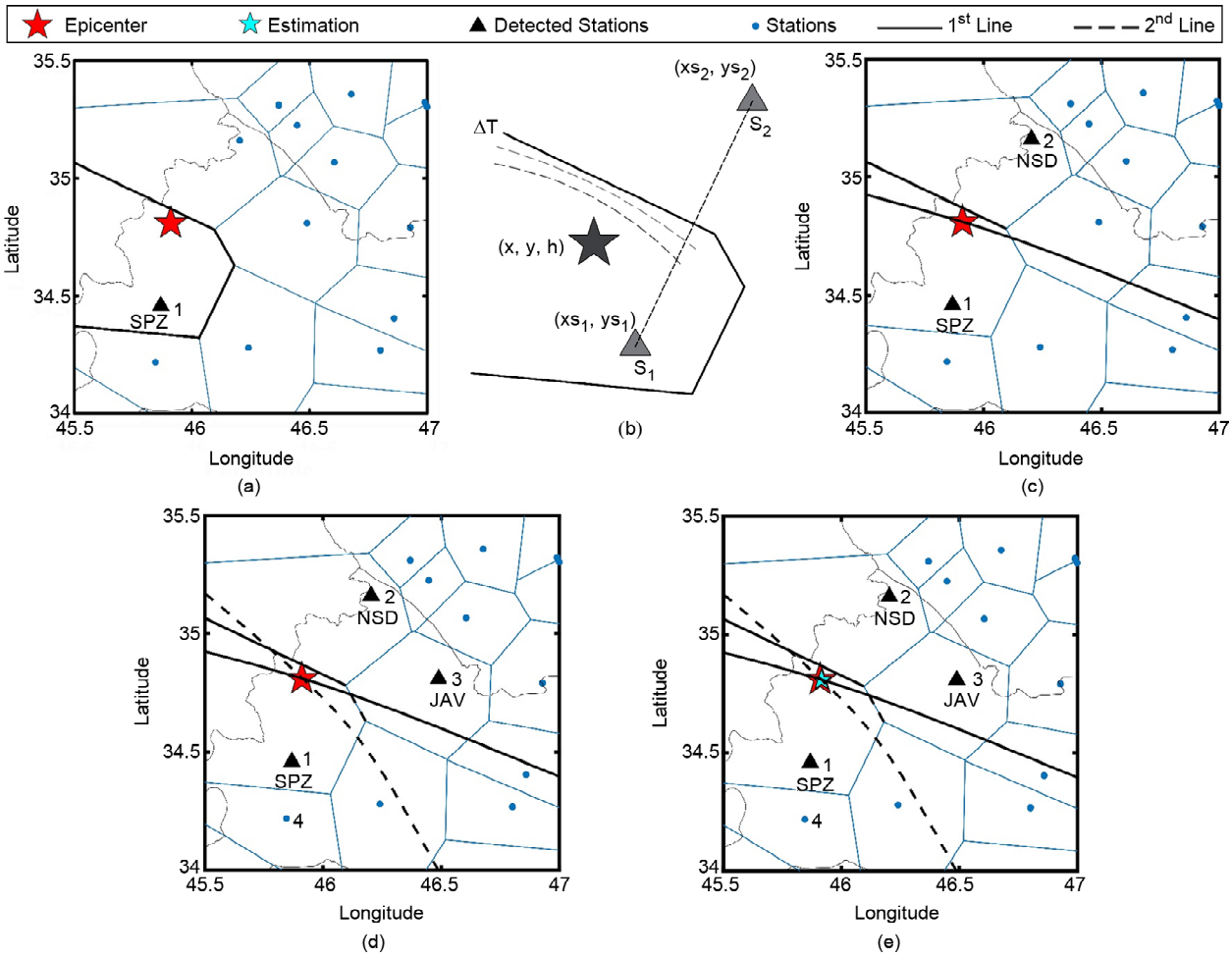

Figure 3. (a) The blue circles show available stations, and red star is the offline determined epicentre (the point of comparison) and the blue lines are corresponding to Voronoi subdivisions in the Sarpol-e Zahab region. The black triangle is the first station that received the P-wave, and the corresponding subdivision polygon is shown by black dash lines; (b) (x, y, h) represents the coordinates of the measured hypocentre, (x_{S1}, x_{S2}) shows the coordinates of the first station that detected the P-wave, and (x_{S2}, y_{S2}) is the coordinates of the second station where the P-wave was recorded. After the second station triggers, the boundary line of the first and second stations begins to bend and shrink toward the first station using Equation (1), as shown by dashed lines hyperbolics; (c) the second station has been triggered and the borderline of the first and the second stations has been considered as an indicator to determine the location of the earthquake. The boundary line has been converted to a hyperbolic curve by using Equation (1), and the time lag between the P-wave arrival to the first and the second stations. The estimated location of the earthquake is located somewhere at a point on this hyperbolic curve; (d) the first and the third stations' borderline is considered as the indicator to determine the location of the earthquake. This boundary line is converted to a hyperbolic curve (dashed line) using Equation (1) and the time lag between stations 1 and 3 and (e) Sarpol-e Zahab earthquake location using the first three stations receiving the P-wave, and the comparison with the BHRC coordinates.

years 1995-2019, which is equal to 10 km (for this purpose, IRSC [29] data has been used, last accessed 14/12/2019). As seen in Figure (3b), the two dashed line hyperbolics (Voronoi subsurface boundary) are tilted toward the first station, which was calculated by Equation (1), using different values of Δt [26].

$$\sqrt{(x-x_{S2})^2+(y-y_{S2})^2+h^2}-\sqrt{(x-x_{S1})^2+(y-y_{S1})^2+h^2}=V_P\Delta t \quad (1)$$

where V_P and Δt indicate, respectively, the velocity of the P-wave and the P-wave time travel to reach the second station from the first station (the difference in P-picking between the two stations).

2.2. Locating the Epicentre Considering the First two Stations to Receive the P Wave

After the *P* wave is observed at the second station, the epicentre is somewhere between the first and second stations. In addition, by taking into account the information we obtained from the previous step, that the location of the earthquake is inside the subdivision polygon of the first station, it is concluded that the epicentre is in the area between the first station and the boundary between the first and second stations. The exact epicentre can

be determined by the time difference of the P wave reaching the first and second stations. In this way, the first and the second stations' boundary is considered as an indicator, from which the epicentre can be estimated, as seen in Figure (3c). Then, to achieve a more accurate estimate, the boundary between the first and the second stations is converted to a hyperbolic tilted toward the first station with the time interval $(\Delta t_1 = t_{P2} - t_{P1})$ using Equation (1) as seen in Figure (3c). In other words, it means that the epicentre is located at a point on this hyperbolic curve.

2.3. Locating the Epicentre with the First Three Stations to Receive the P Wave

A third station is needed to determine an accurate epicentre. As seen in Figure (3d), after triggering the third station, the steps in the previous section are repeated, this time for the first and the third stations. Similar to the previous step, the boundary for the first and the third stations is considered the second indicator line, as shown in Figure (3d). Then, the time interval between the P-wave arrival from the first station to the third station is calculated, $\Delta t_2 = t_{P3} - t_{P1}$. Then the boundary between these two stations is converted to a hyperbolic curve, which tilts toward the first station, by using Equation (1). Eventually, the two hyperbolae intersect at least once, considering the earthquake's estimated epicentre, as seen in Figure (3d). It is worth mentioning that a local coordinate system is used to obtain the epicentre (see also [26]).

Using the first three stations to receive the P-wave, an epicentre of 34.809 N and 45.915 E was obtained, as shown in Figure (3e). This is only 0.5 km from the location reported by the BHRC [4], i.e. 34.81N and 45.91E. As seen in Table (1), this indicates the high accuracy of the method used here for real-time application. However, the reliability of the applied method needs to be investigated in other severe earthquakes and also by considering different sources of uncertainties. Besides, one of the drawbacks of this method is the lack of an accurate estimate of the epicentre for earthquakes that occur outside the Voronoi network. In this case, the more distant the epicentre, the larger the error will be. Of course, this can be effectively solved by accurately identifying the location of geological faults, and by optimising and installing extra recording stations.

Table 1. The coordinates of the epicentre and depth announced by various institutions as well as the results of the current study for the Sarpol-e Zahab earthquake.

Reference	Depth	Longitude	Latitude
BHRC	18	45.91	34.81
IGTU[1]	18.1	45.76	34.77
NEIC[2]	19	45.95	34.91
The Present Study	18.14	45.915	34.809

1. Institute of Geophysics, Tehran University

2. National Earthquake Information Center

3. Estimating the Hypocentral Depth (h)

In determining the location of an earthquake, especially within an EEWS, estimating the focal depth is particularly important since it significantly impacts the severity of an earthquake. The severity directly impacts the decision of whether to trigger a warning or not (and potentially leading to a false alarm). To estimate the depth in an EEWS, we need to know more than what was required to determine the epicentre of the earthquake. This additional information can either be due to the arrival of the P wave at a fourth station (4P condition) or the arrival of the S wave at the first station (3P1S condition) [26]. This second condition is used here for further investigations. Equation (2) shows the relationship for the focal length of the first station. This equation is highly dependent on the velocity of the S and P waves and the time it takes to reach the first station [26].

$$r_1 = \frac{V_P V_S}{V_P - V_S}\left(t_{S1} - t_{P1}\right) \tag{2}$$

V_S and V_P are, respectively, the velocity of the S-wave and P-wave. It is necessary to have information about the arrival times of the S and P waves to solve Equation (2). Therefore, the algorithm introduced by Kalkan [1-3] and its supplemental MATLAB file has been used to pick the arrival times of the P and S phases automatically. For better detection, the arrival time of the P-wave is extracted from the vertical component of the acceleration record (Z component), in which the P-wave is more energetic, and the arrival time of the S-wave is extracted from the horizontal component of the acceleration record (E component), where the

S wave is more energetic. As seen in Figure (4), for the first station, the P arrival time is 14.73 s and the S arrival time is 19.90 s.

Equation (3) is used to calculate the earthquake's depth, h, in kilometres. In this equation, depth is a function of the hypocentral distance from the first station. The distance of the first station to the epicentre can be calculated using the estimated location from the previous steps and the availability of its coordinates (Δ_1^2). The focal depth is calculated through Equation (3):

$$h = \sqrt{r_1^2 - \Delta_1^2} \tag{3}$$

By using Equation (3), the earthquake depth was estimated as 18.14 km. As a result, the earthquake hypocentre was calculated, using the first three stations receiving the P-wave and the first station receiving the S-wave. Table (1) shows the results obtained from this method with the locations announced by different institutions.

It is worth mentioning that we have decided to use two criteria to trigger/not-trigger the alert: (1) the recorded PGA corresponding to the S-wave arrival (it is equal to 0.09 g in Figure (4) in the present study) is equal or greater than 0.05 g, which roughly corresponds to macroseismic intensity *V*[30] (a reasonable engineering judgement for initiation of structural damage) and (2) the estimated depth is less than 50 km. These two simple criteria ensure that non-destructive motions do not trigger the EEWS.

4. Possibility of a Hypothetical EEWS in the Region

The potential benefit of establishing an EEWS in this region is investigated in this section by assessing the potential warning times provided by a hypothetical system based on the existing seismic network. The resulting warnings could be used for both people and automated systems to improve the risk management as well as the resilience of societies [31]. The end-user mitigation actions could include warning people to move to a safer location and more sophisticated measures like automatic braking of high-speed trains. These actions could also include shutting down fuel pipelines to avoid fires and reduce potential damage to industrial operations, which is crucial for industries dealing with dangerous substances (e.g. oil refining), with possible disastrous secondary damage to the environment. Such industries are common in this region of great hydrocarbon resources.

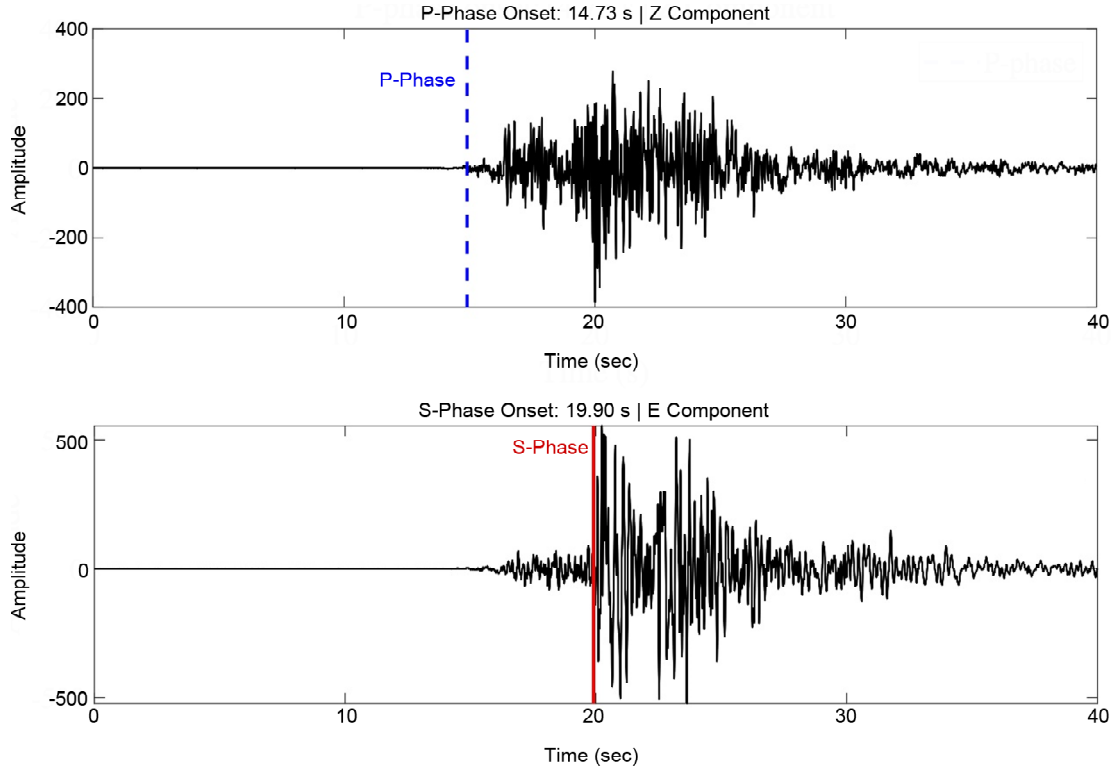

Figure 4. The arrival time of the P-wave from the vertical component of the acceleration record (Z component) is equal to 14.73 seconds, and the arrival time of the S-wave from the horizontal component of the acceleration record (E component) is equal to 19.90 seconds (the first station record) [1-3].

The P and S wave velocities from the crustal structure model of Abbassi et al. [32] for this region are used, and a constant 4s processing and warning lag time is assumed [33-34]. The wave travel time for each distance is calculated based on the P and S wave velocities and the depths of each crustal layer.

A hypothetical EEWS is assumed in the study region, and the data from the four nearest recording stations to the epicentre are taken into consideration. The current study estimates how much warning time would be available if such a system existed in the region. For this purpose, the warning times are calculated using Equation (4) [35]:

$$\Delta t = \frac{\sqrt{(E_{User}^2 + z^2)}}{v_s} - \frac{\sqrt{(E_{Sensor}^2 + z^2)}}{v_p} - t_{decision} - t_{transmission} \quad (4)$$

where Δt is the warning time, E_{Sensor} and E_{User} are the epicentral distances of the first detection site and of the user's location, respectively. Z is the focal depth of the earthquake (in km) and v_p and v_s are the P and S-wave average velocity (in km/s), respectively. $t_{decision}$ and $t_{transmission}$ are two additional times taking into account the time needed for data processing and that for data transmission (in s). $t_{transmission}$ (1 s in this study) is more related to technological limitations while the decision time (3 s in this study) is related to how sure the decision-maker wants to be of the earthquake's destructivity [35]. It is worth mentioning that the alarm is triggered when at least four stations detect the P wave to minimise potential false alarms. In this study, to obtain more realistic warning times, a 1D velocity model [32] is used to compute the travel time in each layer. The time of arrival of the wave from the hypocentre at the considered location is obtained by adding the travel time in each layer.

The observed MMI and the closest available recorded PGA, both versus the estimated warning time using this approach, are shown, respectively, in Figure (5) top and bottom, which indicate that, for example, 20 s of warning time is often available for locations where the observed MMI was VI, which corresponds to the strong shaking and the onset of damage. As seen in Figure (6), the warning times provided for the neighbouring counties in Iran, including the capital, Tehran, and the adjacent countries, Turkey and Iraq, are also significant. The warning time is about 21 s in Kermanshah and Sanandaj cities, and it increases up to 131 s in the case of the Tehran metropolitan area. These warning times are reasonable for emergency actions for an earthquake-resilient society.

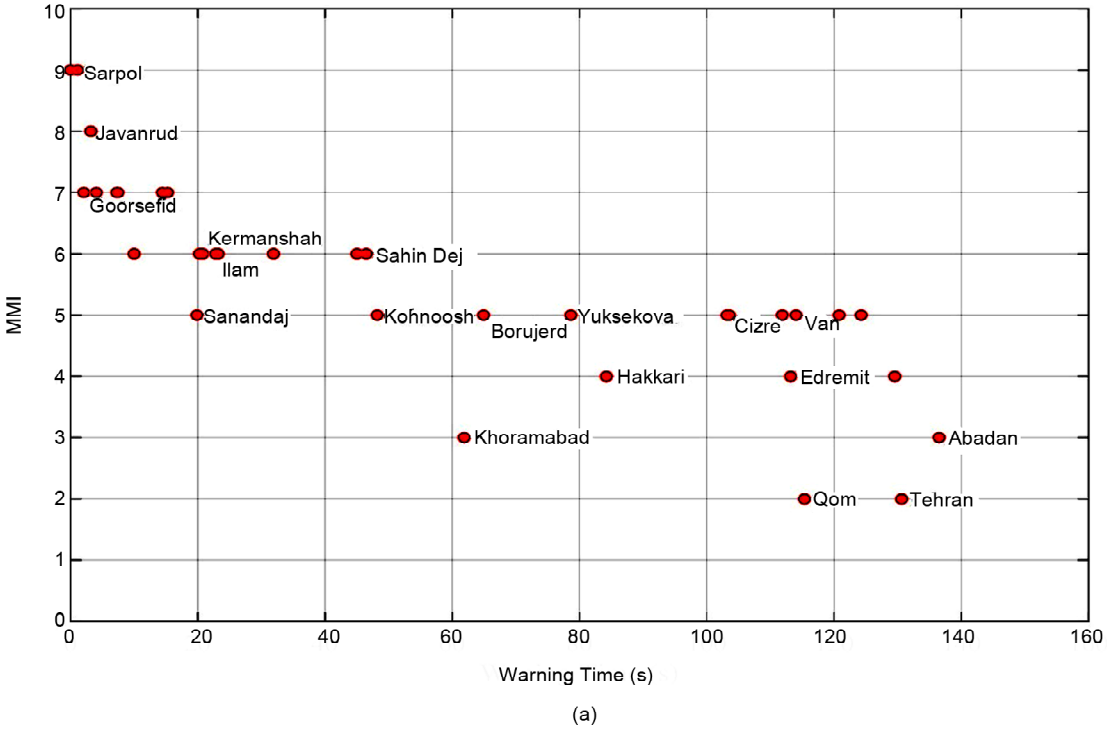

(a)

Figure 5. (a) MMI versus estimated warning time and (b) the closest available recorded PGA versus estimated warning time, for major cities in Figure (6).

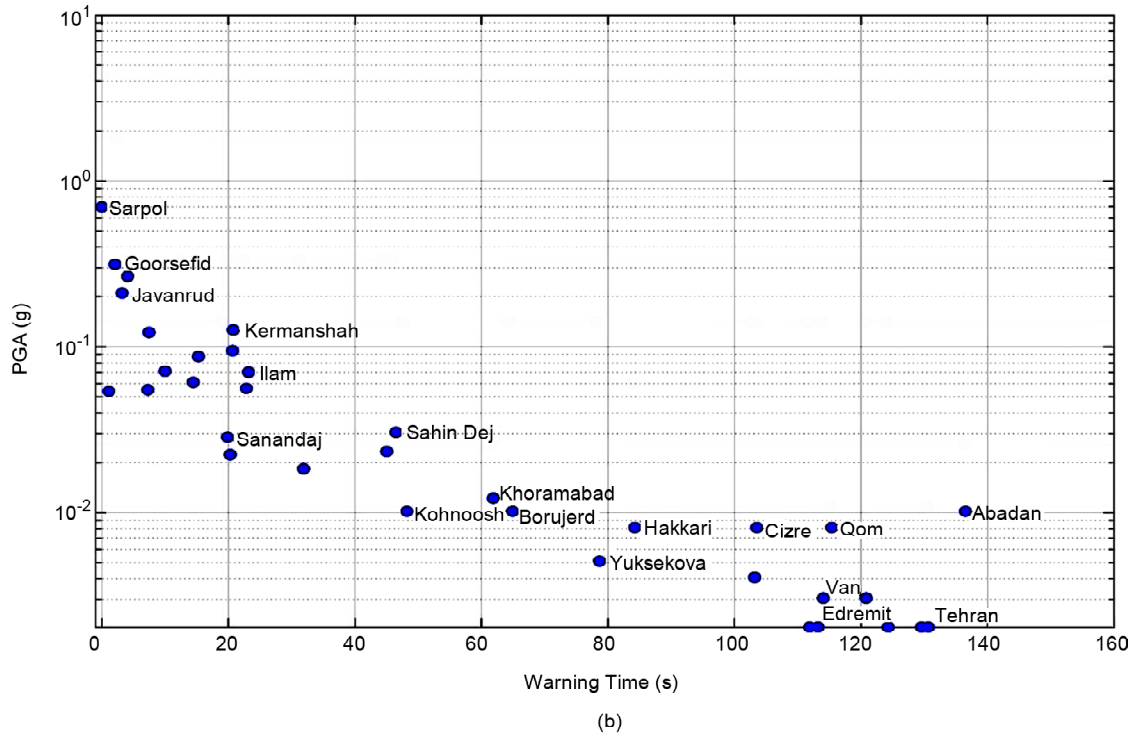

(b)

Figure 5. Continue.

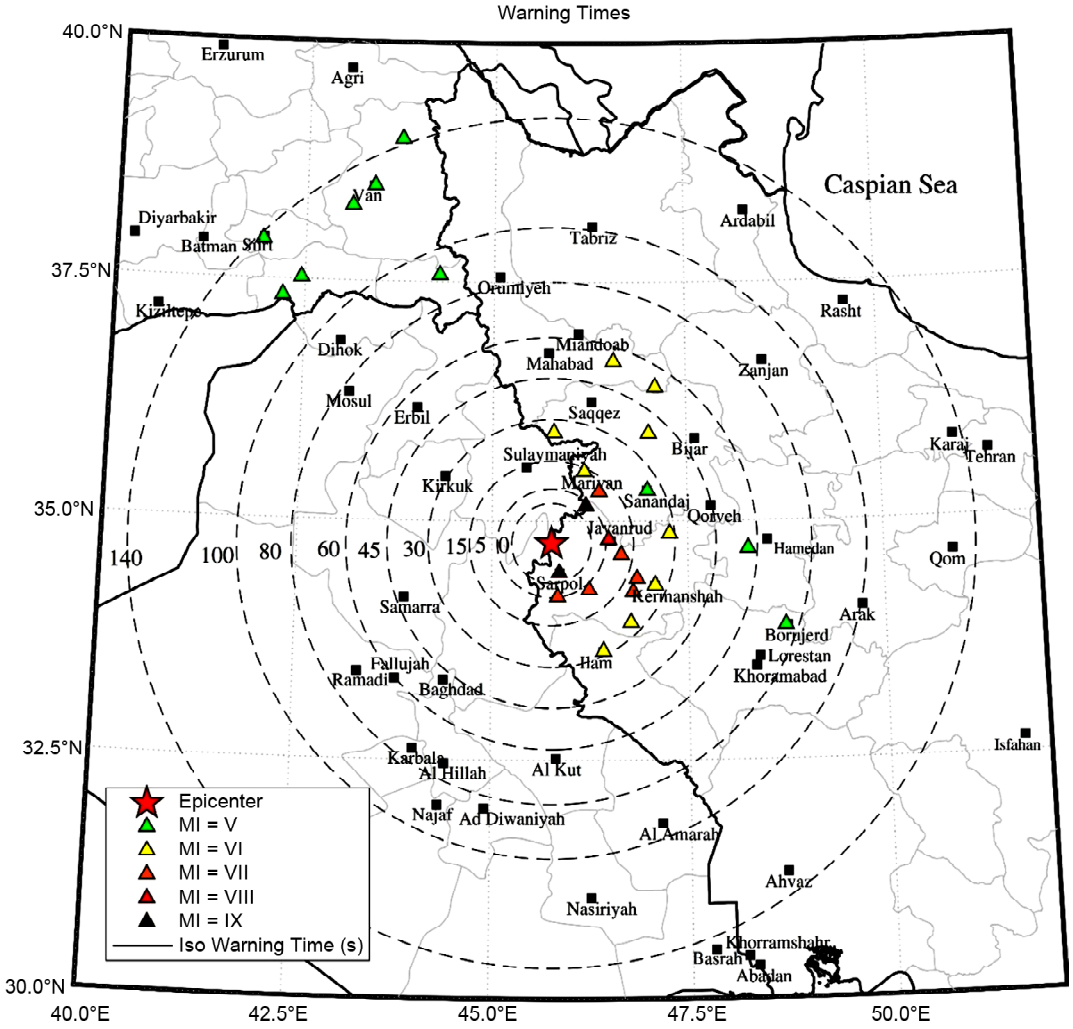

Figure 6. The estimated warning times (in seconds) for western Iran and neighbouring countries.

5. Conclusions

In the present article, the continuous evolution of the Voronoi method has been employed by gradually reducing the area around the first triggering station to locate the Sarpol-e Zahab earthquake, which occurred near the Iraq-Iran border. The real-time epicentre for the Sarpol-e Zahab earthquake, by using only the first three stations, has been estimated at only 0.5 km from that obtained using a more advanced, offline method and more data. This indicates the high accuracy of the employed method to locate the epicentre in a real-time framework, making it a promising approach for EEW.

Furthermore, the depth of the Sarpol-e Zahab earthquake is estimated using the algorithm introduced by Kalkan [1-3] to determine the arrival times of the P and S seismic phases. As a result, the earthquake depth was estimated, using the first three stations receiving the P-wave and the first station receiving the S-wave. A difference of only 0.1 km from offline calculations was observed.

Finally, a hypothetical EEWS in the western region of Iran was proposed. The recorded data from the Sarpol-e Zahab earthquake was used to test the applicability of this hypothetical EEWS. The possible warning times for locations in Iran and the neighbour counties of Iraq and Turkey were estimated using a regional crustal structural model and realistic lag times. The results show that the warning times varied between 17 s and 128 s for the main cities in the region. The results also show the benefit of establishing an appropriate early warning system in the region to increase social resilience to earthquakes, despite the inherent uncertainties, which need further research. We believe that the present study adds to the already available technical knowledge on EEW for the study region. The multi-national issues of warning remain challenging to address, and, as is often the case, these are made worse by politics. It is a national security risk to warn another nation of an imminent natural disaster, especially given the negative consequences due to a potential false alarm.

Finally, it is worth emphasising that the proposed approach has revealed promising results, at least for the given case study with the pre-mentioned assumptions. However, more investigation is necessary for other severe earthquakes with different characteristics. In addition, several other aspects should be considered for a holistic EEWS, e.g. distinguishing noisy recorded waveforms and waveforms from distant stations.

Acknowledgements

The third and fourth authors were supported by the European Union's Horizon 2020 research and innovation programme under grant agreement No 821046, project TURNkey (Towards more Earthquake-resilient Urban Societies through a Multi-sensor-based Information System enabling Earthquake Forecasting, Early Warning and Rapid Response actions).

Conflict of Interest

There are no conflicts of interest associated with this research.

References

1. Kalkan, E. (2016) An automatic P-phase arrival-time picker. *Bulletin of the Seismological Society of America*, **106**(3), 971-986.

2. Kalkan, E. (2019a) An automated P-phase Arrival Time Picker with SNR output: <https://www.mathworks.com/matlabcentral/fileexchange/57729-an-automated-p-phase-arrival-time-picker-with-snr-output>.

3. Kalkan, E. (2019b) An Automated S-phase Arrival Time Picker with SNR Output: <https://www.mathworks.com/matlabcentral/fileexchange/70343-an-automated-s-phase-arrival-time-picker-with-snr-output>.

4. BHRC (2017) Sarpolezahab - 2017: <https://smd.bhrc.ac.ir/Portal/en/Search/BigQuakes>.

5. Cremen, G. and Galasso, C. (2020) Earthquake early warning: Recent advances and perspectives. *Earth-Science Reviews*, **205**, 103184.

6. Berberian, M. (2013) Early earthquake detection and warning alarm system in Iran by a telegraph operator: A 116-year-old disaster prevention attempt. *Seismological Research Letters*, **84**(5), 816-819.

7. Heidari, R., Shomali, Z.H., and Ghayamghamian, M.R. (2013) Magnitude-scaling relations using period parameters τc and τp max, for Tehran

region, Iran. *Geophysical Journal International*, **192**(1), 275-284.

8. Heidari, R. (2016) Quick estimation of the magnitude and epicentral distance using the P wave for earthquakes in Iran. *Bulletin of the Seismological Society of America*, **106**(1), 225-231.

9. Mahood, M. (2018) Rapid estimating epicentral distance and magnitude from a single seismic record of Sarpol-e Zahab earthquake. *Journal of Seismology and Earthquake Engineering*, **20**(2), 29-36.

10. Nakamura, Y. (1988) On the urgent earthquake detection and alarm system (UrEDAS). *Proc. of the 9th World Conference on Earthquake Engineering*, **7**, 673-678, Japan.

11. Nakamura, Y. (2005) Earthquake early warning and derailment of Shinkansen train at the 2004 Niigataken-Chuetsu earthquake. *Environmental Systems Research*, **28**, 115-115.

12. Shahbazi, P. and Mansouri, B. (2018) Loss modeling for 2017 Sarpol-e Zahab Earthquake. *Journal of Seismology and Earthquake Engineering*, **20**(4), 69-80.

13. Farzanegan, E., Pourmohammad Shahvar, M., Eshaghi, A., Mirsanjari, M., Abdollahi, H., and Mirzaee, H. (2017) *Report of the November 12, 2017 Sarpol-e Zahab, Kermanshah Province Earthquake*. Iran Strong Motion Network (ISMN).

14. USGS (2018) M 7.3 - 29km S of Halabjah, Iraq: <https://earthquake.usgs.gov/earthquakes/eventpage/us2000bmcg/map-dyfi-responses-10km=true&shakemap-intensity=false>.

15. Anderson, K.R. (1981) Epicentral location using arrival time order. *Bulletin of the Seismological Society of America*, **71**(2), 541-545.

16. Kanamori, H. (1993) Locating earthquakes with amplitude: Application to real-time seismology. *Bulletin of the Seismological Society of America*, **83**(1), 264-268.

17. Zhou, H.W. (1994) Rapid three-dimensional hypocentral determination using a master station method. *Journal of Geophysical Research: Solid Earth*, **99**(B8), 15439-15455.

18. Odaka, T., Ashiya, K., Tsukada, S.Y., Sato, S., Ohtake, K., and Nozaka, D. (2003) A new method of quickly estimating epicentral distance and magnitude from a single seismic record. *Bulletin of the Seismological Society of America*, **93**(1), 526-532.

19. Rydelek, P. and Pujol, J. (2004) Real-time seismic warning with a two-station subarray. *Bulletin of the Seismological Society of America*, **94**(4), 1546-1550.

20. Horiuchi, S., Negishi, H., Abe, K., Kamimura, A., and Fujinawa, Y. (2005) An automatic processing system for broadcasting earthquake alarms. *Bulletin of the Seismological Society of America*, **95**(2), 708-718.

21. Satriano, C., Lomax, A., and Zollo, A. (2008) Real-time evolutionary earthquake location for seismic early warning. *Bulletin of the Seismological Society of America*, **98**(3), 1482-1494.

22. Ma, Q. (2008) *Study and Application on Earthquake Early Warning*. Institute of Engineering Mechanics, China Earthquake Administration, Harbin, 124-134.

23. Wald, D.J. (2020) Practical limitations of earthquake early warning. *Earthquake Spectra*, **36**(3), 1412-1447.

24. Grasso, V.F., Beck, J.L., and Manfredi, G. (2007) Seismic early warning systems: Procedure for automated decision making. *Earthquake Early Warning Systems*, 179-209, Springer, Berlin, Heidelberg.

25. Allen, R.M. (2004) 'Rapid magnitude determination for earthquake early warning'. In: The many facets of seismic risk, edited by G. Manferedi et al., 15-24, Univ. Degli Studi di Napoli "Federico II", Naples, Italy.

26. Jin, X., Zang, H.C., Li, J., Wei, Y.X., and Ma, Q. (2012) Research on continuous location method used in earthquake early warning system. *Chinese Journal of Geophysics*, **55**(2), 150-165.

27. Afsari, N., Sodoudi, F., Gheitanchi, M.R., and Kaviani, A. (2010) Moho depth variations and Vp/Vs ratio in Northwest of Zagros (Kermanshah region) using teleseismic receiver functions. *Journal of Geoscience*, **19**(74), 45-50.

28. Afsari, N., Sodoudi, F., Farahmand, F.T., and Ghassemi, M.R. (2011) Crustal structure of northwest Zagros (Kermanshah) and Central Iran (Yazd and Isfahan) using teleseismic PS converted phases. *Journal of Seismology*, **15**(2), 341-353.

29. IRSC (2019) Iranian Seismological Center: <http://irsc.ut.ac.ir/bulletin.php>.

30. Caprio, M., Tarigan, B., Worden, C.B., Wiemer, S., and Wald, D.J. (2015) Ground motion to intensity conversion equations (GMICEs): A global relationship and evaluation of regional dependency. *Bulletin of the Seismological Society of America*, **105**(3), 1476-1490.

31. Gasparini, P., Manfredi, G., and Zschau, J. (Eds.) (2007) *Earthquake Early Warning Systems*. Berlin: Springer.

32. Abbassi, A., Nasrabadi, A., Tatar, M., Yaminifard, F., Abbassi, M.R., Hatzfeld, D., and Priestley, K. (2010) Crustal velocity structure in the southern edge of the Central Alborz (Iran). *Journal of Geodynamics*, **49**(2), 68-78.

33. Allen, R.M., Brown, H., Hellweg, M., Khainovski, O., Lombard, P., and Neuhauser, D. (2009) Real-time earthquake detection and hazard assessment by ElarmS across California. *Geophysical Research Letters*, **36**(5).

34. Brown, H.M., Allen, R.M., Hellweg, M., Khainovski, O., Neuhauser, D., and Souf, A. (2011) Development of the ElarmS methodology for earthquake early warning: Realtime application in California and offline testing in Japan. *Soil Dynamics and Earthquake Engineering*, **31**(2), 188-200.

35. Kuyuk, H.S. (2015) Warning time analysis for emergency response in Sakarya City, Turkey against possible Marmara earthquake. *Journal of Structural Mechanics*, **1**(3), 134-139.